

Nitrogen local electronic structure in Ga(In)AsN alloys by soft-x-ray absorption and emission: Implications for optical properties

V. N. Strocov,¹ P. O. Nilsson,² T. Schmitt,³ A. Augustsson,³ L. Gridneva,³ D. Debowska-Nilsson,² R. Claessen,¹
A. Yu. Egorov,⁴ V. M. Ustinov,⁴ and Zh. I. Alferov⁴

¹*Experimentalphysik II, Universität Augsburg, D-86135 Augsburg, Germany*

²*Department of Physics, Chalmers University of Technology and Göteborg University, SE-41296 Göteborg, Sweden*

³*Department of Physics, Uppsala University, Ångström Laboratory, Box 530, S-75121 Uppsala, Sweden*

⁴*A.F. Ioffe Physico-Technical Institute, 194021 St. Petersburg, Russia*

(Received 10 March 2003; revised manuscript received 3 September 2003; published 27 January 2004)

Soft-x-ray-emission and -absorption spectroscopies with their elemental specificities are used to determine the local electronic structure of N atoms in Ga(In)AsN diluted semiconductor alloys (N concentrations about 3%) in view of applications of such materials in optoelectronics. Deviations of the N local electronic structure in Ga(In)AsN from the crystalline state in GaN are dramatic in both valence and conduction bands. In particular, a depletion of the valence-band maximum in the N local charge, taking place at the N impurities, appears as one of the fundamental origins of reduced optical efficiency of Ga(In)AsN. Incorporation of In in large concentrations forms In-rich N local environments such as In₄N which become the main recombination centers in GaInAsN. Furthermore, a **k** character of some valence and conduction states, despite the random-alloy nature of Ga(In)AsN, manifests itself in resonant inelastic x-ray scattering.

DOI: 10.1103/PhysRevB.69.035206

PACS number(s): 78.70.En, 78.70.Dm, 71.55.-i, 78.55.Cr

I. INTRODUCTION

Ga(In)AsN semiconductor alloys are new promising optoelectronic materials, whose potential applications range from efficient solar cells to laser diodes operating in the long-wavelength range ($\lambda \sim 1.3 \mu\text{m}$) which fits the transparency window of optofibers used in local networks. A remarkable property of the Ga(In)AsN alloys is an extremely strong dependence of the band-gap width E_g on the N content, characterized by a giant bowing coefficient with $dE_g/dx = 15\text{--}20 \text{ eV}$ (see, e.g., Ref. 1). This figure is more than one order of magnitude larger compared to the conventional III-V alloys, which suggests that physical mechanisms to narrow the band gap are quite different. A disadvantage of the Ga(In)AsN alloys is however their low optical efficiency compared to conventional III-V alloys such as GaAs and AlAs.

Physics of Ga(In)AsN and related alloys has been under intense study during the last few years (see Refs. 1–5, and references therein). Due to a strong difference in the N and As scattering potentials, insertion of N atoms into the host lattice results in a giant perturbation of the electronic structure and formation of fundamentally new electronic states such as resonant impurity states. Their hybridization with the host states in the conduction band strongly perturbs and shifts these states to lower energies, which narrows the band gap. Different local environments of N atoms such as isolated impurities, N-N pairs, and various clusters form different states hybridizing with each other. Because of the immense complexity of such a system no exhaustive theoretical treatment exists up to now. Different approaches such as the empirical pseudopotential supercell method,^{1,2} first-principles pseudopotential method,³ and band anticrossing model⁴ often give conflicting predictions. Moreover, their

experimental verification is complicated by significant scatter in the experimental results depending on the sample preparation. Despite significant advances in understanding of the band-gap narrowing in Ga(In)AsN alloys, mechanisms responsible for degradation of their optical efficiency are still not completely clear.

A vast amount of the experimental data on the Ga(In)AsN and similar alloys has been obtained using optical spectroscopies such as photoluminescence (PL) and electroreflectance (see, e.g., a compilation of references in Ref. 1). However, they are largely restricted to the band-gap region, and give in general only bare positions of the energy levels without any direct information about spatial localization or orbital character of wave functions. Such an information can be achieved by soft-x-ray-emission (SXE) and soft-x-ray-absorption (SXA) spectroscopies with their specificity on the chemical element and orbital character (see, e.g., a recent review in Ref. 6). Although their energy resolution, intrinsically limited by the core-hole lifetime, never matches that of the optical spectroscopies, they give an overall picture of the electronic structure on the energy scale of the whole valence band (VB) and conduction band (CB). Moreover, as the orbital selection rules involve the core state and thus engage the VB and CB states different from those engaged in optical transitions, the soft-x-ray spectroscopies give a complementary view of the electronic structure. Because of the small atomic concentrations in diluted alloys such as Ga(In)AsN, and small cross section of the SXA and SXE processes, these experiments require the use of third-generation synchrotron radiation sources, providing soft x rays at high intensity and brilliance, and high-resolution SXE spectrometers with multichannel detection.⁷

Extending our pilot work,⁸ we here present experimental SXE and SXA data on Ga(In)AsN diluted alloys, which unveil the local electronic structure of N impurities through the

whole VB and CB. This yields fundamental physics of Ga(In)AsN and related alloys, in particular, electronic structure origins of their limited optical efficiency, effect of In on the N local environments and electronic structure, and \mathbf{k} character of some VB and CB states coupled by resonant inelastic x-ray scattering (RIXS).

II. EXPERIMENTAL PROCEDURE AND RESULTS

A. Sample growth

The Ga(In)AsN samples were grown by molecular-beam epitaxy (MBE) at an EP-1203 machine (Russia) equipped by solid-phase Ga, In, and As sources and a radio frequency plasma N source. Details of the growth procedure and sample characterization are given elsewhere.⁹ Briefly, the growth was performed on a GaAs(001) substrate at 430 °C in As-rich conditions. The active layer in our GaAsN and GaInAsN samples was grown, respectively, as GaAs_{0.97}N_{0.03} with a thickness of 200 Å, and In_{0.07}Ga_{0.93}As_{0.97}N_{0.03} with a thickness of 240 Å (growth of thicker layers was hindered by phase segregation). The concentrations of In and N were checked by high-resolution x-ray rocking curves. A buffer layer between the substrate and the Ga(In)AsN active layer, and a cap layer on top of it were grown each as a 50-Å-thick AlAs layer sandwiched between two 50-Å-thick GaAs layers. Such an insertion of wide band-gap AlAs is a usual method to increase the PL intensity by confining the carriers in the Ga(In)AsN layer. Moreover, a high-temperature annealing of the grown structure can be performed after deposition of AlAs in the cap layer without desorption of GaAs. Such an annealing lasts about 10 min at 700–750 °C. The resulting improvement of the Ga(In)AsN layer crystal quality typically increases the PL intensity by a factor of 10–20.

The annealing effect on the local environments of N atoms is less clear. The N impurities are known to interact with each other due to long-range lattice relaxation and long tails of their wave functions down to N concentrations of 0.1%,¹ which translates to a characteristic interaction length of 60 Å. We expect that on this length scale the annealing can promote energetically favorable N local environments. In GaAsN such environments are, for example, (100)-oriented N pairs.¹ In the GaInAsN quaternary alloy the situation is more complicated: whereas as-grown samples have nearly random distributions of In and N atoms with a significant fraction of InAs clusters having small chemical bond energy, the annealing should promote formation of In-N bonds, providing better lattice match to the GaAs substrate and thus minimizing the strain energy.¹⁰ In any case, on a length scale larger than the N interaction length the annealing should improve homogeneity of the N concentration. This is of paramount importance, in particular, for our experiment because due to the giant bowing coefficient of Ga(In)AsN any fluctuations of the N concentration should result in significant fluctuations of the electronic structure^{11,12} and therefore in smearing of spectral structures.

B. SXE/SXA measurements

The SXE/SXA experiments were performed in MAX lab, Sweden, at the undulator beam line I511-3 equipped with a

modified SX-700 plane grating monochromator and a high-resolution Rowland-mount grazing incidence spectrometer.¹³ SXE/SXA measurements employed the N 1s core level at ≈ 400 eV.

The SXA spectra were recorded in the fluorescence yield (FY), because due to the thick cap layer the electron yield did not show any N 1s absorption structure. The measurements were performed in partial FY using the SXE spectrometer operated slitless. It was adjusted at a photon energy window centered at the N *K*-emission line and covering an interval, in the first order of diffraction, from some 320 to 470 eV. The signal was detected with the spectrometer position-sensitive detector as the integral fluorescence within this energy window. Interestingly, usual measurements in the total FY (detected with a microchannel plate detector in front of the sample) returned considerably different spectra. This is possibly because the total FY is more susceptible to irrelevant contributions due to higher-order incident light and low-energy photoelectron bremsstrahlung fluorescence, significant with our low N concentrations in the host material. As the partial FY measurements are characterized by significant intensity loss due to smaller acceptance angle of the spectrometer, we operated the monochromator at an energy resolution of 0.45 eV full width at half maximum (FWHM) [the N 1s lifetime broadening is about 0.1 eV (Ref. 14)].

The synchrotron-radiation excited SXE spectra were measured, in view of the low cross section of the SXE process and small N concentration, with the monochromator resolution lowered to ~ 1.5 eV and to ~ 0.5 eV for the off-resonance and resonant spectra, respectively. The spectrometer was operated with a spherical grating of 5 m radius and 400 lines/mm groove density in the first order of diffraction, providing a resolution of ~ 1.2 eV. The signal from the position-sensitive detector was aberration corrected using third-order polynomial fitting and normalized to the total illuminated area in each channel on the detector. Normal data acquisition time was 2–5 h per spectrum. Despite the cap layer we could also see a N signal under 3.5-keV electron-beam excitation, although on top of strong bremsstrahlung background, but this was not suitable for resonant measurements.

Energy calibration of the spectrometer was performed in absolute photon energies employing the Ni L_1 , $L_{\alpha_{1,2}}$, and L_{β_1} lines seen in the second order of diffraction. Abberations in the dispersion direction of the position-sensitive detector were corrected by setting an energy scale as a function of the channel number using second-order polynomial fitting. Based on the elastic peaks in SXE spectra, the monochromator was then calibrated in the same absolute energy scale with an accuracy of about ± 0.15 eV.

C. Experimental results

Our experimental N 1s SXA spectra (measured in the partial FY) (Ref. 15) and off-resonant SXE spectra (excitation energy of 420 eV, well above the absorption threshold) of the GaAs_{0.97}N_{0.03} and Ga_{0.93}In_{0.07}As_{0.97}N_{0.03} samples are shown in Fig. 1 (*upper panel*). The binding-energy scale is set relative to the VB maximum (VBM) determined, roughly,

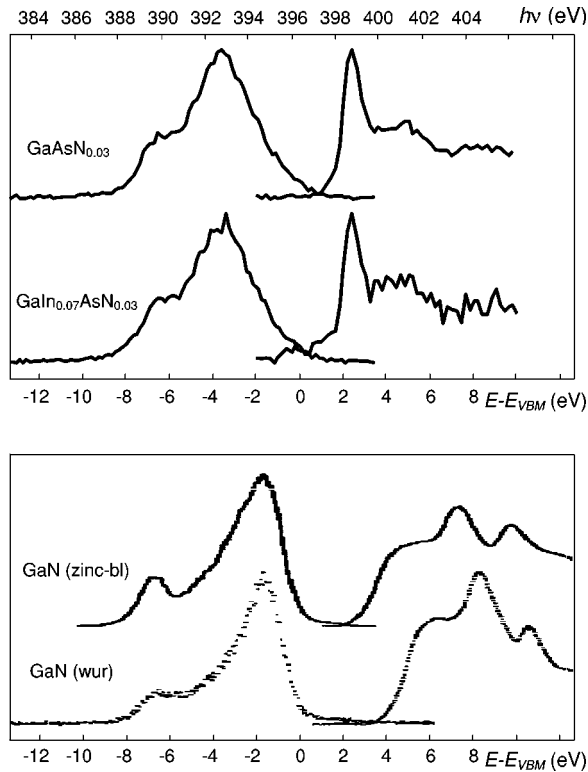


FIG. 1. (*Upper panel*) Experimental N $1s$ off-resonant SXE (excitation energy 420 eV) and SXA spectra of $\text{GaAs}_{0.97}\text{N}_{0.03}$ and $\text{Ga}_{0.93}\text{In}_{0.07}\text{As}_{0.93}\text{N}_{0.03}$, reflecting the N local p -DOS through the VB and CB; (*lower panel*) the corresponding spectra of crystalline GaN in the zinc blende (Ref. 14) and wurtzite structures (Ref. 21) shown as a reference. The SXE spectral maximum for Ga(In)AsN is strongly shifted to lower energies compared to the crystalline state, resulting in depletion of the N local charge in the VBM which reduces optical efficiency.

by linear extrapolation of the SXE spectral leading edge. We intentionally give the spectra without denoising to facilitate judgement of the significance of the spectral structures compared to the noise level. Recent supercell calculations by Persson and Zunger¹⁶ are in good agreement with our experimental results.

Recent SXA data on $\text{GaAs}_{0.97}\text{N}_{0.03}$ by Lordi *et al.*¹⁷ which appeared after initial submission of this paper, are consistent with our results (apart from some energy shift which is presumably because their energy scale was affected by the monochromator calibration). Previous SXA data by Soo *et al.*¹⁸ suffer from worse experimental resolution and sample quality.

Local environments of the N atoms in Ga(In)AsN are polymorphic, corresponding to isolated impurities and various clusters.¹ Applying random statistics, the concentration ratio of the pair and higher-order N clusters to the total number of N atoms is given by $1 - (1 - x)^m$, where x is the N concentration and $m = 4$ the number of the nearest anions in the zinc blende lattice. With our N concentrations of 3% this ratio is only 11.5%. Therefore, our SXE/SXA spectra characterize mainly the isolated N impurities.

III. DISCUSSION

A. Overall picture of the electronic structure

The experimental SXA and off-resonance SXE spectra in Fig. 1 reflect, by the dipole selection rules requiring that the orbital quantum number l be changed by ± 1 , the p component of the density of states (DOS) locally in the N core region. The p component, by analogy with crystalline GaN,¹⁴ should in fact dominate the total DOS through the whole VB and CB region. Core excitonic effects are presumably less significant because the direct recombination peak¹⁹ does not show up in our SXE spectra. Splitting of the VBM into the light- and heavy-hole subbands due to a strain imposed by the GaAs substrate,²⁰ being about a few tenths of eV is below our experimental resolution.

It is instructive to compare our Ga(In)AsN spectra to the corresponding spectra of crystalline GaN. They are reproduced in Fig. 1 (*lower panel*) in the binding-energy scale determined in the same way as for Ga(In)AsN. The spectra of GaN in the metastable zinc blende structure, which has the same N coordination as Ga(In)AsN, were measured by Lawniczka-Jablonska *et al.*¹⁴ and those of wurtzite GaN by Stagaescu *et al.*²¹ Apart from the CB shift, the spectra of the two crystalline forms are similar in overall shape. They are well understood in terms of the local orbital-projected DOS and band structure.^{14,22}

Comparison of the SXE/SXA data on Ga(In)AsN to those on the two GaN crystalline structures shows the following.

(1) In the VB, the overall shape of the SXE signal for Ga(In)AsN is similar to crystalline GaN. However, the spectral maximum is strongly shifted towards the VB interior, with the leading edge at the VBM being much less steep (which has important implications for optical efficiency, see below). This is not a resolution effect, because the reference spectra of crystalline GaN were taken at close resolution figures (around 0.8 eV for zinc blende GaN and 1.1 eV for wurtzite GaN). Our experimental data demonstrate thus that the VB electronic structure undergoes, contrary to the common point of view, significant changes upon incorporation of N atoms into GaAs. Interestingly, our SXE spectrum did not show any structure due to hybridization with the Ga $3d$ states at ~ 19 eV below the VBM, found in wurtzite GaN.^{21,23}

(2) In the CB, the differences are radical. The leading peak of the SXA spectrum for Ga(In)AsN rises immediately at the CB minimum (CBM) and has much larger amplitude compared to the leading shoulderlike structure in the spectra of crystalline GaN. The energy separation between the VB and CB states for Ga(In)AsN is smaller, which correlates with smaller fundamental band gap.

On the whole, the observed differences of the Ga(In)AsN spectra to crystalline GaN manifest that the local electronic structure of the N atoms in the Ga(In)AsN random alloy is radically different from that in the regular GaN lattice.

Although further theoretical analysis is required to interpret our experimental data in detail, we can tentatively assign the leading SXA peak to the $t_2(L_{1c})$ derived perturbed host state which, according to the calculations by Kent and Zunger on GaAsN,¹ has the strongest N localization in the

CBM region. This assignment is corroborated by the resonant SXE data (see below) which reveals the L character of the leading SXA peak.

It should be noted that the dipole selection rules in SXE/SXA, inherently involving transitions from and to the core level, project out the states from the VB and CB, which can differ from those projected out by the optical transitions between the VB and CB states themselves. For example, delocalized states can give only a small contribution to the SXE/SXA signal due to relatively small overlap with the core state, but they can strongly overlap with each other and give a strong PL signal. Our SXA data give explicit examples of this: The $a_1(\Gamma_{1c})$ derived states near the CBM (see Ref. 1) are not seen in the SXA spectrum due to the weaker N localization compared to the $t_2(L_{1c})$ states, but in optical spectroscopies they manifest themselves as the intense E^- transitions. On the other hand, the $t_2(L_{1c})$ states are not seen in the optical spectra due to unfavorable matrix elements, but show up as a prominent SXA peak. Moreover, the energy separation between the VB and CB states in the SXE/SXA spectra gives only an upper estimate for the fundamental band gap, because weakly localized N states as well as Ga and As derived states are not seen. Therefore, the SXE/SXA spectroscopies give a view of the VB and CB complementary to that by optical spectroscopies.

B. Charge depletion in the VBM: Origin of reduced optical efficiency

The vast body of optical spectroscopy data on Ga(In)AsN evidences that the optical efficiency sharply drops upon incorporation of the smallest N concentrations into GaAs, and then decreases further with increase of the N molar fraction (see, e.g., a compilation in Ref. 5). This is most pronounced for GaAsN, where the PL intensity loss towards N concentrations of 5% is at least 50 times as compared to GaAs. Exact origins of such a dramatic efficiency degradation are not completely clear. Supercell calculations in Ref. 24 suggest that about 30% of the GaAs efficiency is lost due to gradual smearing of VBM and CBM in their Γ character, which results in reduction of the optical transition matrix element. However, this effect is by far weaker compared to the experimental degradation. Another known origin is relatively poor structural quality of Ga(In)AsN layers epitaxially grown on GaAs. This is due to, first, low growth temperatures which are used with large N concentrations to promote high N uptake and, second, some lattice mismatch between Ga(In)AsN and GaAs. However, the first problem can be alleviated by postgrowth high-temperature annealing, and the second by tuning the In concentration in GaInAsN which allows matching the GaAs lattice constant. Although the PL intensity from lattice-matched GaInAsN layers does increase by a factor about 5 compared to GaAsN, this still remains by far low compared to GaAs. Moreover, the structural quality does not explain the efficiency drop at the smallest N concentrations.

Our SXE/SXA results unveil another origin of the optical efficiency degradation in the very electronic structure. By virtue of the N localization of the CBM wave function¹

the N impurities act as the main recombination centers in Ga(In)AsN. At the same time, the local valence charge at the N impurities is shifted off the VBM. This appears immediately from comparison of our experimental SXE spectra of Ga(In)AsN with those of crystalline GaN, which are in fact representative of GaAs by virtue of qualitatively similar valence DOS of these materials²⁵ (direct measurements on GaAs are hindered by very low fluorescence yield of As in the soft-x-ray region). Such a charge depletion in the VBM, equivalent to reduction of the VBM wave-function amplitude, results in a weak overlap of the CBM and VBM wave functions at the N impurities, which immediately reduces efficiency of the N impurities as radiative recombination centers. This VBM depletion effect, characteristic of isolated N impurities, is one of the fundamental origins of the reduced optical efficiency of Ga(In)AsN. Being in play already at the smallest N concentrations, it immediately explains the initial efficiency drop, whereas further efficiency degradation with increase of N concentration is presumably through the structural quality effects.

To explain the observed VBM charge depletion, in Ref. 8 we suggested a VBM charge transfer off the N atoms in Ga(In)AsN compared to GaN (in Ref. 16 our this statement was misinterpreted as a charge transfer to As, but N has larger electronegativity). In fact, the charge transfer is more likely to take place not in space but in energy towards deeper valence states, which is supported by recent computational analysis of Persson and Zunger.¹⁶ Physically, the local electronic structure of the N impurities in the GaAs lattice appears somewhere in between that of the crystalline state and isolated atoms. The observed DOS peaked near the VB center can therefore be viewed as a transitional case between the DOS of extended band states piling up near the band edges and the singularitylike DOS of isolated atoms at the VB center.

Formation of N local environments different from the isolated impurities can be suggested as a way to increase the optical efficiency of Ga(In)AsN. For example, in multi-atomic N local environments such as clusters of Ga-separated N atoms the wave functions may become closer to crystalline GaN with its DOS piling up at the VBM. Based on the random statistics, the cluster concentration should increase with the total N concentration. Alternatively, the N local environments can be changed by replacing some neighbor Ga atoms by different cations.

C. Effect of In

Quaternary GaInAsN alloys, where some Ga atoms are replaced by In, allow improvement of the optical efficiency by a factor about 5. This is predominantly due to two factors: a better lattice match of GaInAsN layers to the GaAs substrate, which improves their structural quality, and electron confinement effects connected with concentration fluctuations.¹¹ We here endeavored investigation whether the incorporation of In also causes any favorable changes in the electronic structure.

At relatively low In concentrations, evolution of the N local electronic structure is evidenced by comparison of the

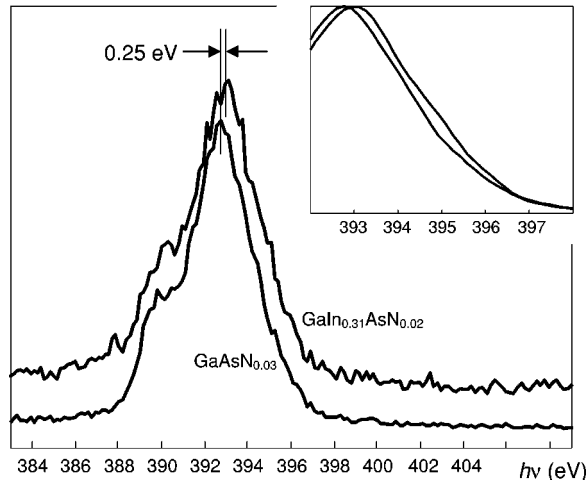


FIG. 2. Experimental off-resonant N $1s$ SXE spectrum of In-rich $\text{Ga}_{0.69}\text{In}_{0.31}\text{As}_{0.98}\text{N}_{0.02}$ compared to $\text{GaAs}_{0.93}\text{N}_{0.03}$. The inset details the spectral leading edges (Gaussian smoothed with FWHM of 0.6 eV) which suggest improved optical efficiency of In-rich N local environments.

$\text{Ga}_{0.93}\text{In}_{0.07}\text{As}_{0.97}\text{N}_{0.03}$ and $\text{GaAs}_{0.97}\text{N}_{0.03}$ experimental spectra in Fig. 1. Surprisingly, the comparison shows no notable changes within the experimental statistics, either in the spectral shapes or in energies of the spectral structures. This evidences that the following takes place at low In concentrations:

(1) The N atoms reside mostly in In-depleted local environments such as Ga_4N and possibly $\text{In}_1\text{Ga}_3\text{N}$ where the presence of only one In atom in four nearest neighbors should not change the N local electronic structure significantly. This experimental finding seriously questions results of recent Monte Carlo simulations¹⁰ which predict predominance of In-rich N local environments such as $\text{Ga}_1\text{In}_3\text{N}$ and In_4N , at least with low In concentrations. Any effect connected with insufficient high-temperature annealing of our samples can be ruled out, as evidenced by stabilization of PL spectra already after 5 min of annealing. Our results are corroborated by Fourier-transform infrared (FTIR) absorption measurements by Alt *et al.* (see, e.g., Ref. 26) who also find mostly Ga_4N local environments which, moreover, are not affected by annealing. On the other hand, FTIR results by Kurtz *et al.*²⁷ suggest preferential formation of In-rich environments with annealing. Such a contradiction reveals that evolution of the N local environments critically depends on the growth procedure.

(2) The absence of any significant electronic structure changes compared to GaAsN suggests that the optical efficiency improvement in GaInAsN is exclusively due to the structural and electron confinement effects.

To force formation of In-rich N local environments, we have grown a sample of $\text{Ga}_{0.69}\text{In}_{0.31}\text{As}_{0.98}\text{N}_{0.02}$ (170-Å-thick active layer) where the In/N concentration ratio is much increased (the decrease in bare N concentration is presumably less important because interaction of the isolated N impurities in such diluted alloys should be weak). The experimental SXE spectrum of $\text{Ga}_{0.69}\text{In}_{0.31}\text{As}_{0.98}\text{N}_{0.02}$, measured under the same off-resonance conditions as in Fig. 1, is also shown in

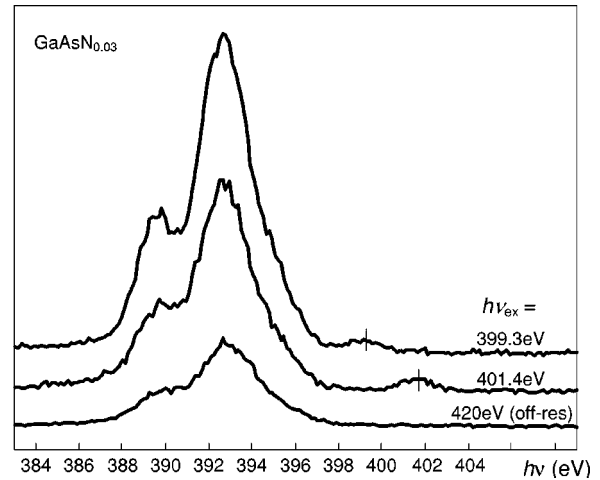


FIG. 3. Resonant SXE spectra with the indicated excitation energies compared to an off-resonant spectrum. The elastic peaks are marked by vertical ticks. The resonant intensity enhancement in the VB bottom manifests a \mathbf{k} -conserving RIXS process.

Fig. 2. Now the spectral maximum is shifted by some 0.25 eV to higher energies compared to $\text{GaAs}_{0.97}\text{N}_{0.03}$, indicating changes in the N local electronic structure caused by In-rich N environments.

The observed VB shift to higher energies is accompanied by a shift of the CB to lower energies, as seen in the recent XAS data on $\text{Ga}_{0.7}\text{In}_{0.3}\text{As}_{0.97}\text{N}_{0.03}$ from Ref. 17. Such VB and CB shifts towards each other, associated with In-rich N local environments, have important implications for the radiative recombination:

(1) By virtue of the local band-gap narrowing, these environments become the main recombination centers in GaInAsN.

(2) Both holes and electrons become confined in In-rich regions, formed by statistical fluctuations of In concentration, to increase the optical efficiency of GaInAsN.¹¹

To see whether the observed changes in the VB affect the optical efficiency within the above VBM depletion mechanism, we examined closely the VBM region (inset in Fig. 2). The shift of the spectral maximum is definitely larger than that of the VBM (although its exact location requires better statistics). This indicates certain charge accumulation at the VBM compared to $\text{GaAs}_{0.97}\text{N}_{0.03}$, and thus increase of the optical efficiency of In-rich N local environments compared to Ga_4N . The observed accumulation seems though rather subtle to explain the increase in GaInAsN wholly, and most of it still resides with the structural and electron confinement effects.

D. \mathbf{k} conservation in the RIXS process

Resonant phenomena were investigated on the GaAsN prototype alloy. Figure 3 shows resonant SXE spectra measured with excitation energies near the two dominant SXA structures in Fig. 1 compared to a nonresonant spectrum measured well above the absorption threshold. The spectra are normalized to the integral excitation flux, which was registered from the photocurrent at a gold mesh inserted after the refocusing mirror.

Intriguingly, not only does the intensity of the resonant spectra increase in this RIXS process, but also the shoulder at the VB bottom scales up and becomes a distinct narrow peak at a binding energy of ~ 7.4 eV. This reveals states near the VB bottom effectively overlapping with states near the CB bottom into which the core electron is excited.

Despite the random-alloy nature of Ga(In)AsN, the observed effect can be interpreted in terms of momentum conservation, which appears in the RIXS process due to coupling of absorption and emission in one single event (see, e.g., Refs. 6,28,29, and references therein). At first glance, the very concept of momentum, strictly speaking, collapses in a random alloy due to the lack of translational invariance. However, it can be revived through a spectral decomposition

$$\psi^N(\mathbf{r}) = \sum_{\mathbf{k}} C_{\mathbf{k}} \phi_{\mathbf{k}}^{\text{GaAs}}(\mathbf{r})$$

of the N-localized wave function $\psi^N(\mathbf{r})$ over the Bloch waves $\phi_{\mathbf{k}}^{\text{GaAs}}(\mathbf{r})$ of the unperturbed GaAs lattice, each having a well-defined wave vector \mathbf{k} .^{1,30} Then the first SXA peak is due to the $t_2(L_{1c})$ state, whose decomposition is dominated by \mathbf{k} from the L point in the Brillouin zone of GaAs.¹ The VB bottom, by analogy with the zinc blende GaN band structure,³¹ should also be dominated by the L point. These VB and CB states then effectively overlap in the RIXS process, blowing up the SXE signal in the VB bottom as observed in the experiment. Our resonant data demonstrate thus, to our knowledge for the first time, a possibility for the \mathbf{k} -conserving RIXS phenomenon in random alloys.

IV. CONCLUSION

Local electronic structure of N atoms in Ga(In)AsN diluted semiconductor alloys (N concentrations about 3%) has been determined using SXE/SXA spectroscopies with their elemental specificity. The experimental N $1s$ off-resonance

SXE spectra and SXA spectra yield the local p DOS of N impurities through the whole VB and CB, complementing information about the band-gap region achieved by optical spectroscopies. The experimental results demonstrate dramatic differences of the N local electronic structure in Ga(In)AsN from that in the crystalline GaN state. A few peculiarities have immediate implications for optical properties.

(1) The N impurities as radiative recombination centers are characterized by depletion of the local charge in the VBM due to charge transfer towards deeper valence states, which reduces overlap with the CBM states. This is one of the fundamental origins of the reduced optical efficiency of Ga(In)AsN. Formation of different N local environments can improve the efficiency.

(2) Whereas incorporation of In in small concentrations has an insignificant effect on the N local electronic structure, large In concentrations result in formation of In-rich N local environments. Due to the VB and CB shifts towards each other such environments become the main recombination centers in GaInAsN.

Furthermore, the experimental resonant SXE spectra reveal, despite the random-alloy nature of Ga(In)AsN, a \mathbf{k} -conserving RIXS process which couples valence and conduction states having the same L character.

ACKNOWLEDGMENTS

We are grateful to A. Zunger and C. Persson for valuable comments and communicating their computational results before publication. We thank S. Butorin for his advise on SXE data processing, J. Guo for help with preliminary experiments, and G. Cirlin for valuable discussions. The work in the Ioffe institute was supported by the NATO Science for Peace Program (Project No. SfP-972484) and Russian Foundation for Basic Research (Project No. 02-02-17677).

¹P.R.C. Kent and A. Zunger, Phys. Rev. Lett. **86**, 2613 (2001); Phys. Rev. B **64**, 115208 (2001).

²T. Mattila, S.-H. Wei, and A. Zunger, Phys. Rev. B **60**, R11245 (1999).

³A. Al-Yacoub and L. Bellaiche, Phys. Rev. B **62**, 10847 (2000).

⁴K.M. Yu, W. Walukiewicz, W. Shan, J.W. Ager III, J. Wu, E.E. Haller, J.F. Giesz, D.J. Friedman, and J.M. Olson, Phys. Rev. B **61**, R13337 (2000).

⁵I.A. Buyanova, W.M. Chen, and B. Monemar, MRS Internet J. Nitride Semicond. Res. **6**, 2 (2001).

⁶A. Kotani and S. Shin, Rev. Mod. Phys. **73**, 203 (2001).

⁷J. Nordgren and J. Guo, J. Electron Spectrosc. Relat. Phenom. **110-111**, 1 (2000).

⁸V.N. Strocov, P.O. Nilsson, A. Augustsson, T. Schmitt, D. Debowska-Nilsson, R. Claessen, A.Yu. Egorov, V.M. Ustinov, and Zh.I. Alferov, Phys. Status Solidi B **233**, R1 (2002).

⁹A.Yu. Egorov, D. Bernklau, B. Borchert, S. Illek, D. Livshits, A. Rucki, M. Schuster, A. Kaschner, A. Hoffmann, Gh. Dumitras, M.C. Amann, and H. Riechert, J. Cryst. Growth **227-228**, 545 (2001).

¹⁰K. Kim and A. Zunger, Phys. Rev. Lett. **86**, 2609 (2001).

¹¹A.M. Mintairov, T.H. Kosel, J.L. Merz, P.A. Blagnov, A.S. Vlasov, V.M. Ustinov, and R.E. Cook, Phys. Rev. Lett. **87**, 277401 (2001).

¹²K. Matsuda, T. Saiki, M. Takahashi, A. Moto, and S. Takagishi, Appl. Phys. Lett. **78**, 1508 (2001).

¹³J. Nordgren, G. Bray, S. Cramm, R. Nyholm, J.-E. Rubensson, and N. Wassdahl, Rev. Sci. Instrum. **60**, 1690 (1989).

¹⁴K. Lawniczak-Jablonska, T. Suski, I. Gorczyca, N.E. Christensen, K.E. Attenkofer, R.C.C. Perera, E.M. Gullikson, J.H. Underwood, D.L. Ederer, and Z. Liliental Weber, Phys. Rev. B **61**, 16 623 (2000).

¹⁵SXA spectra measured in the total FY (see our Ref. 8) reproducibly show up a pronounced peak in some 2 eV above the leading absorption peak, which may be due to structure in the low-energy bremsstrahlung or elastic reflectivity.

¹⁶C. Persson and A. Zunger, Phys. Rev. B **68**, 035212 (2003).

¹⁷V. Lordi, V. Gambin, S. Friedrich, T. Funk, T. Takizawa, K. Uno, and J.S. Harris, Phys. Rev. Lett. **90**, 145505 (2003).

¹⁸Y.L. Soo, S. Huang, Y.H. Kao, J.G. Chen, S.L. Hulbert, J.F.

- Geisz, S. Kurtz, J.M. Olson, S.R. Kurtz, E.D. Jones, and A.A. Allerman, *Phys. Rev. B* **60**, 13605 (1999).
- ¹⁹A. Agui, S. Shin, C. Wu, K. Shiba, and K. Inoue, *Phys. Rev. B* **59**, 10 792 (1999).
- ²⁰Y. Zhang, A. Mascarenhas, H.P. Xin, and C.W. Tu, *Phys. Rev. B* **61**, 4433 (2000).
- ²¹C.B. Stagarescu, L.-C. Duda, K.E. Smith, J.H. Guo, J. Nordgren, R. Singh, and T.D. Moustakas, *Phys. Rev. B* **54**, R17335 (1996).
- ²²W.R.L. Lambrecht, S.N. Rashkeev, B. Segall, K. Lawniczak-Jablonska, T. Suski, E.M. Gullikson, J.H. Underwood, R.C.C. Perera, J.C. Rife, I. Grzegory, S. Porowski, and D.K. Wickenden, *Phys. Rev. B* **55**, 2612 (1997).
- ²³L.-C. Duda, C.B. Stagarescu, J. Downes, K.E. Smith, D. Korakakis, T.D. Moustakas, J.H. Guo, and J. Nordgren, *Phys. Rev. B* **58**, 1928 (1998).
- ²⁴L. Bellaiche, S.-H. Wei, and A. Zunger, *Phys. Rev. B* **56**, 10233 (1997).
- ²⁵J.R. Chelikowski, T.J. Wagener, J.H. Weaver, and A. Jin, *Phys. Rev. B* **40**, 9644 (1989).
- ²⁶H.Ch. Alt, A.Yu. Egorov, H. Riechert, J.D. Meyer, and B. Weidemann, *Physica B* **308-310**, 877 (2001).
- ²⁷S. Kurtz, J. Webb, L. Gedvilas, D. Friedman, J. Geisz, J. Olson, R. King, D. Joslin, and N. Karam, *Appl. Phys. Lett.* **78**, 748 (2001).
- ²⁸S. Eisebitt, J. Lüning, J.-E. Rubensson, A. Settels, P.H. Dederichs, W. Eberhardt, S.N. Patitsas, and T. Tiedje, *J. Electron Spectrosc. Relat. Phenom.* **93**, 245 (1998).
- ²⁹J.A. Carlisle, E.L. Shirley, L.J. Terminello, J.J. Jia, T.A. Callcott, D.L. Ederer, R.C.C. Perera, and F.J. Himpsel, *Phys. Rev. B* **59**, 7433 (1999).
- ³⁰L.-W. Wang, L. Bellaiche, S.-H. Wei, and A. Zunger, *Phys. Rev. Lett.* **80**, 4725 (1998).
- ³¹J.P. Lewis, K.R. Glaesemann, G.A. Voth, J. Fritsch, A.A. Demkov, J. Ortega, and O.F. Sankey, *Phys. Rev. B* **64**, 195103 (2001).